

# THE USE OF HIGH-RESOLUTION SATELLITE IMAGERY FOR DERIVING GEOTECHNICAL PARAMETERS APPLIED TO LANDSLIDE SUSCEPTIBILITY

L. Blesius<sup>a,\*</sup>, F Weirich<sup>b</sup>

<sup>a</sup> San Francisco State University, Department of Geography, San Francisco, CA 94132, USA - lblesius@sfsu.edu

<sup>b</sup> IHR Hydrosience and Engineering, and Department of Geoscience, University of Iowa, Iowa City, IA 52240, USA  
– Frank-Weirich@uiowa.edu

WG I/2, I/4, IV/2, IV/3, VII/2

**KEY WORDS:** Landslide susceptibility, Geotechnical parameters, Quickbird

## ABSTRACT:

In order to mitigate hazards of mass failure, the first step is the identification of potentially unstable slopes, resulting in a landslide susceptibility map. Satellite imagery is an important component in the derivation of critical parameters. Susceptibility maps can be constructed in a variety of ways, including multivariate statistics, heuristic models, and geotechnical models. Each method has been shown to successfully identify hazardous slopes. The method employing geotechnical data has attracted attention, but the problem is a lack of critical parameters such as angle of internal friction or cohesion. These data may be available for few selected slopes, but typically not over a spatially coherent area. This severely limits the use of geotechnical models for landslide susceptibility maps. This study addresses the potential of using remote sensing and in particular high-resolution satellite imagery to derive values for important variables such as angle of internal friction and soil cohesion that are necessary for the geotechnical approach and specifically for the application of the infinite slope method to landslide susceptibility assessment. A 2002 Quickbird image was analyzed with respect to land cover, and then reclassified according to specific geotechnical parameters, in particular: cohesion; angle of internal friction; and root cohesion. The latter has been shown to be of high significance in slope stability. The resulting map spatially depicts the factor of safety or F-value over the study area. This map is compared with a 2005 Quickbird image in which multiple failures that occurred after a fire and subsequent rain storms are visible. The correspondence between the F-value map and the Quickbird image is quite visible, but further studies in refining the parameters are needed. This research suggests that satellite images can be successfully used to derive reasonable values for critical parameters in a geotechnical stability model, thereby increasing the utility of the geotechnical approach in landslide susceptibility mapping.

## 1. INTRODUCTION

### 1.1 General Instructions

The determination of areas susceptible to mass failure has been an ongoing area of both basic and applied research in remote sensing and mass movement studies. The mapping of landslide susceptibility is also a critical aspect of efforts to mitigate hazards of mass failure. Satellite imagery plays an important role in these efforts by enabling the identification of critical parameters, for example lithology, land use, and, if stereo imagery is available, elevation and slope. The resulting landslide maps can be divided into two categories – inventory or density maps and susceptibility or hazard maps. The former are typically based on geomorphological fieldwork and/or air photo interpretation (Guzetti et al., 2000) and seek to document the past record of failures. In contrast, hazard or susceptibility maps seek to predict the likelihood of future failures and are prepared by a variety of methodologies, ranging from fuzzy logic (e.g., Saboya et al., 2005), logical or semi-quantitative overlays (e.g., Sarkar and Kanungo, 2004; Moreiras, 2005), to various statistical models (e.g., Chung & Fabbri, 1999; Baeza and Corominas, 2001; Ayalew and Yamagishi, 2005), and geotechnical models (e.g., Borga et al., 1998, Terlien, 1998). While each of these methods has its merits and drawbacks, each has been shown to successfully identify hazardous slopes. In the case of geotechnical models, one of the more significant drawbacks has been limitations in readily available data that the

models require. While ground-based geotechnical data on such parameters as angle of internal friction or cohesion may be available for a few selected slopes, typically they are not available over a spatially coherent area. This and a high spatial variability severely limit the use of geotechnical models for landslide susceptibility maps (Burton et al., 1998). Therefore, to date, the method has not been widely applied.

This study addresses the potential of using remote sensing and in particular high-resolution satellite imagery to derive values for important variables such as angle of internal friction and soil cohesion that are necessary for the geotechnical approach and specifically for the application of the infinite slope method to landslide susceptibility assessment. In most cases, the infinite slope method has been the method of choice for geotechnical landslide susceptibility mapping, because it is easy to implement in a per-pixel evaluation (Van Westen & Terlien, 1996). It can be also readily adapted to include the weight of the vegetation and added cohesion due to roots. For example, it has been shown that reduced soil cohesion due to deforestation can result in an increased area subject to shallow landslides (Wu and Sidle, 1995). Moreover, this approach can be also applied to other parameters that are not widely measured such as vegetation parameters that may also affect slope stability.

The method described here has been previously applied to the Santa Monica Mountains using SPOT imagery with inconclusive results. While older landslides were not

---

\* Corresponding author.

successfully identified, some existing or recurring landslide areas were identified (Blesius and Weirich, 2006). While lower resolution images like Landsat TM, SPOT, or Aster may not provide enough spatial variability, the newer generation of satellites may be better suited to capture the differences in vegetation and soils to estimate cohesion and internal friction. Quickbird satellite images, for example, have a very high spatial resolution of 2.4m multispectral and 0.6m panchromatic.

## 2. STUDY AREA AND DATA USED

### 2.1 Study area

The study area lies just east of Lake Piru in the Simi Mountains of Ventura County near Santa Clarita, CA (figure 1). It has a Mediterranean climate with average yearly winter temperatures of 10°C and average summer temperatures of 26 °C. The seasonal winter precipitation averages around 450 mm. The area is frequently affected by wild fires, such as the 2003 Piru fire. The area is mountainous with slopes between 30° and 60°. Vegetation is dominated by coastal scrub and chaparral communities. However, coast live oak (*Quercus agrifolia*) is widely present. *Q. agrifolia* typically grows in mesic sites on soils that are well-drained. (Pavlik et al., 1991; Holland, 2005). Chaparral also is found predominantly on the more mesic sites within the southern California provinces (Hanes, 1988). The shrubs of this zone are typically of smaller size and much smaller biomass than chaparral and coast live oak. They generally tend to occupy sites with less seasonal moisture availability and more fine-textured soils, as opposed to chaparral. Often, coastal sage occupies the sites on shales, while chaparral inhabits the sandstone-derived soils (Mooney, 1988). However, the fire history plays a role, because in the past, more of the area has been covered by oaks. Most of the study area has been mapped to the Lodo-Botella families-Rock outcrop association, 30-60% slopes. The Lodo family consists of somewhat excessively drained shallow soils of sandy loam in the upper part of the profile grading into very gravely sandy loam in the lower profile. The Botella family has deeper soils of gravely loam, and is well drained. Both soils developed on shale (NRCS, 2009).

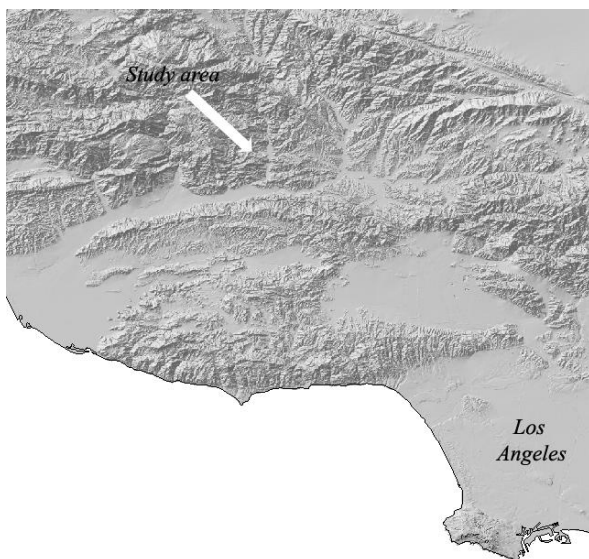


Figure 1: Location of study area.

### 2.2 Data used

Two Quickbird images covering an area of about 16km<sup>2</sup> have a promising characteristic (figures 2 and 3). Image 1 (figure 2) was taken in July 2002 before a large fire in October 2003 and subsequent rainstorms, while image 2 (figure 2) was taken in May 2005 after those events. Both images are clear with no clouds or visible haze effects. The second image displays many significant slope failures in multiple locations. Therefore, this is the ideal situation to evaluate a methodology which attempts to derive critical parameters for a geotechnical landslide susceptibility map.

The 2002 image was used in the analysis and development of the landslide susceptibility map, while the 2005 image was used for an evaluation of the final map and procedure. The spatial resolution of the images is 2.4m. Although a 0.6m panchromatic image was also available, it was not used to create a pan-sharpened image of higher spatial resolution, because the classification of high spatial resolution images can be more challenging due to increased intra-class spectral variability (Yu et al., 2006).



Figure 2. Quickbird image of the study area in the Simi Mountains. The image, designated as image 1, is from 2002.

The procedure involved the creation of orthoimages from the Quickbird data. Orthorectification requires a digital elevation model (DEM). Ideally, this is created from a stereo pair of the original images. However, it can be difficult to develop a reliable DEM from a stereo pair, if the images were not taken within a short time frame, and land-cover has changed within this period. Because this is the case in this instance, a digital elevation model from the US Geological Survey at 10m resolution was used instead.



Figure 3. Quickbird image of the study area in the Simi Mountains. The image, designated as image 2, is from 2005. Note that there are a number of light blue, elongated features. These are the sites of the landslides.

### 3. METHODOLOGY

The procedure involved the creation of orthoimages from the Quickbird data, followed by a land-cover classification. Land cover is an important parameter in many applications, and can be an indicator of various landscape physical parameters. For example, soil maps rely heavily on identification of vegetation indicative of particular soils. In this case, the land cover map was re-analyzed with respect to soil and vegetation properties that are relevant to the infinite slope method. These properties are unit weight of soil, angle of internal friction, and cohesion with respect to the soil properties. With respect to the vegetation, the parameters used were root cohesion and weight of vegetation.

The modified infinite slope function can therefore be written as (Sidle, 1992):

$$F = \frac{c' + c_v + (\gamma z + W_v - \gamma_w d_w) \cos^2 \alpha \tan \phi'}{(\gamma z + W_v) \sin \alpha \cos \alpha} \quad (1)$$

where  $F$  = the factor of safety  
 $c'$  = effective cohesion [kg/m<sup>2</sup>]  
 $c_v$  = root strength of vegetation [kg/m<sup>2</sup>]  
 $\gamma$  = dry weight of soil [kg/m<sup>3</sup>]  
 $z$  = soil depth [m]  
 $W_v$  = weight of vegetation per unit area [kg/m<sup>2</sup>]  
 $d_w$  = depth of water table  
 $u$  = porewater pressure [kg/m<sup>2</sup>]  
 $\alpha$  = slope angle [°].  
 $\phi'$  = effective angle of internal friction [°]

#### 3.1 Image classification

The 2002 image was subjected to an unsupervised classification procedure. Initially 30 classes were differentiated, which

subsequently were merged into 10 classes: (figure 4). Darker green colours show the oak vegetation, medium dark green shades indicate shrub vegetation, while lighter green shades indicate grass cover. Bare areas are shown in light blue.

1. Riparian
2. Oak/shadow
3. Oak
4. Oak/Shrub
5. Shrub
6. Shrub/Grass
7. Grass
8. Grass/Bare
9. Bare/Grass
10. Bare.

It should be noted that most of the bare areas are not landslides. The largest bare area in the right center of the image, for example, is part of Lake Piru during low water levels.

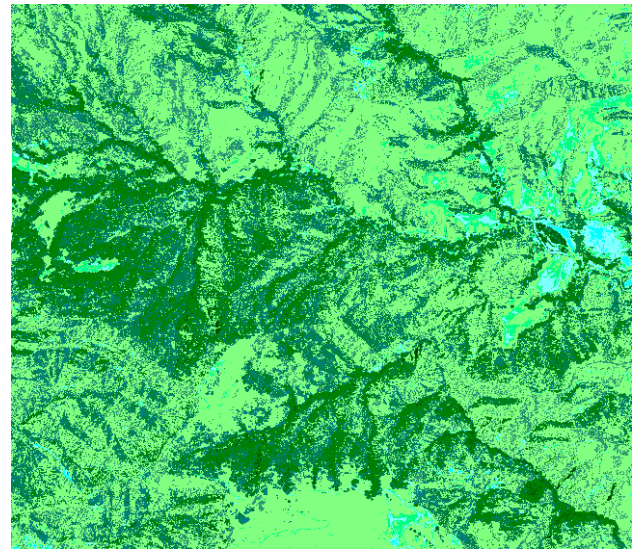


Figure 4. 10 class classification of the 2002 Quickbird image.

#### 3.2 Extraction of geotechnical parameters

The land cover map and the digital elevation model were then employed to estimate soil texture and depth. These soil properties were then combined with a soil library relating texture and depth to the geotechnical parameters of friction angle and cohesion. Similarly, the land cover map was used to derive values for vegetation geotechnical parameters.

**3.2.1 Soil depth** In general, in mountainous terrain, the slope angle can provide a first approximation to soil depth. The steeper the terrain, the more likely soil will erode downslope and the thinner the soil cover. A first approximation of soil depth is therefore the maximum depth for a particular soil times the cosine of the slope angle. Maximum soil depth according to the soil survey (NRCS, 2009) in this area is about 1m.

**3.2.2 Cohesion and angle of internal friction:** The general relationship between the friction angle, density or consistency, and granular soils, especially sands, is well established. Tables can be found in publications such as American Society of Civil Engineers (1994), Das (1997, 1998), or State of California Department of Transportation (1990), who list recommendations for simplified typical soil values and estimations of cohesion based on the soils consistency for cohesive soils. The amount of clay is then used as an indicator for the density of the soil, ranging from soft to hard.

For example, Das (1997) presents a table of different soils from around the world that indicates a correlation between the clay-size fraction and the residual angle of internal friction. A linear relationship can be established, which is illustrated as a graph in figure 5. This function can be taken as a first approximation of friction angle and soil texture for cohesive soils. However, correlations between grain-size distribution and friction angle are really only successful in regions where soils originate from the underlying geologic parent material because different types of clay, while belonging to the same size class, exhibit completely different behaviours – for example, swelling. While relations between plastic limit and friction angle are better established (Terzaghi et al., 1996), this would only be useful if plastic limits were known for the soils within a given area. However, it is more likely that if any soil information is available, it is texture rather than Atterberg limits.

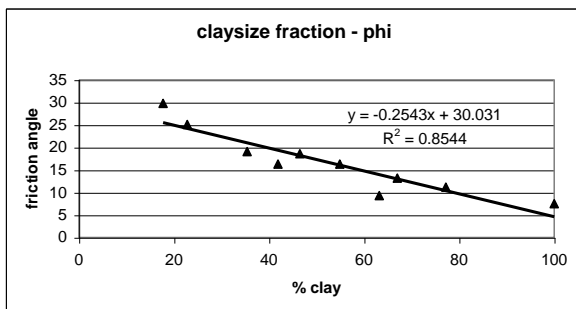


Figure 5: Relationship between claysize fraction and friction angle for different soils. Source: Das (1997)

**3.2.3 Root cohesion and weight of vegetation:** An ongoing challenge to landslide hazard mapping is that in reviewing many reports in the literature it is often surprising to find that areas that should fail, based on conventional calculations of the F-value, have in fact remained stable (e.g. Preston & Crozier, 1999). In many instances this may be due to the strengthening of the soil through the added cohesion provided by roots. The tensile strength of various roots has been estimated to be on the order of 2 – 20KPa for grasses and up to 74 KPa for certain tree species such as alder, *Alnus spec.*, (Wu, 1995). Vetiver grass even has an estimated tensile root strength of between 40 and 120Mpa (Hengchaovanich & Nilaweera, 1996). Other studies report on increased landslide activity once the vegetation has been removed (e.g. Kurupparachchi & Wyrwoll, 1992). Thus, in estimating landslide susceptibility, in many situations it appears important to incorporate this effect into the calculations (see eq. 1).

There have been some reports of vegetative root strength estimated as root cohesion. While specific strength values for

chaparral could not be found, the role of the deep roots of chaparral in reducing the occurrence landslides under chaparral versus failure under riparian woodlands or grassland has been documented (Hellmers et al., 1955, Rice et al., 1969). Moreover, the length and extent of chaparral roots suggests that root cohesion for chaparral is in the upper range, and likely in the 10-20 Kpa range. However, given the wide range in values for chaparral both maximum and minimum values were used. Weight of vegetation is also part of the modified slope stability calculation ( $W_v$  in equation 1). Estimations for average weight range from 2kg/m<sup>2</sup> dry weight for five-year old stands of *Ceanothus megacarpus* to 4.9 kg/m<sup>2</sup> for 21-year old stands (Schlesinger & Gill, 1980), and can reach around 6.0 kg/m<sup>2</sup>. Coastal sage scrub weight is less, about 1.4 kg/m<sup>2</sup> (Mooney, 1988).

**3.2.4 Implementation:** Table 3 list the pertinent values selected for the study site. The riparian corridor vegetation is assumed to be on thicker soils with more clay content, therefore the friction angle would be lower, but cohesive forces are higher. The oaks grow on well-drained soils and have deep roots. It is therefore assumed they are on the Botella family, with gravelly loam in the top horizon, and gravelly clay loam in the lower horizon. The gravel should add to the strength and increase the friction angle, while the clay would contribute to higher cohesive forces.

Class	$\phi$	c (kg/m <sup>2</sup> )	c <sub>v</sub> min (kg/m <sup>2</sup> )	c <sub>v</sub> max (kg/m <sup>2</sup> )
Riparian	21	3600	1250	50
Oak/shadow	24	1800	1050	45
Oak	24	1800	1050	45
Oak/shrub	22	1500	750	40
Shrub	21	1200	350	20
Shrub/grass	20	900	150	10
Grass	19	600	100	1
Grass/Bare	19	300	50	0.5
Bare/Grass	19	100	25	0.1
Bare	20	100	0	0

Table 3: Values used in the infinite slope function.

The grassy vegetation is assumed to be a part of the Lodo family. It is less deep and consists of sandy loam at the top, with a subhorizon of very gravelly sandy loam and very cobbly sandy loam. Therefore lower values for angle of internal friction and cohesion were used. The shrub vegetation is considered to be in between the oak and grass type communities.

### 3.3 Results and discussion

The result of the analysis is shown in figure 6 using both maximum estimated root cohesion and saturated conditions, i.e. the soil is filled to its infiltration capacity. The red areas indicate an F-value of 1, meaning that they are in motion when these conditions prevail. These areas do coincide with areas that experienced sliding as evidenced on the 2005 image (figure 3). Orange and yellow area indicate slopes whose F-value is close to 1. They may not have experienced sliding, but the map suggests they are susceptible.

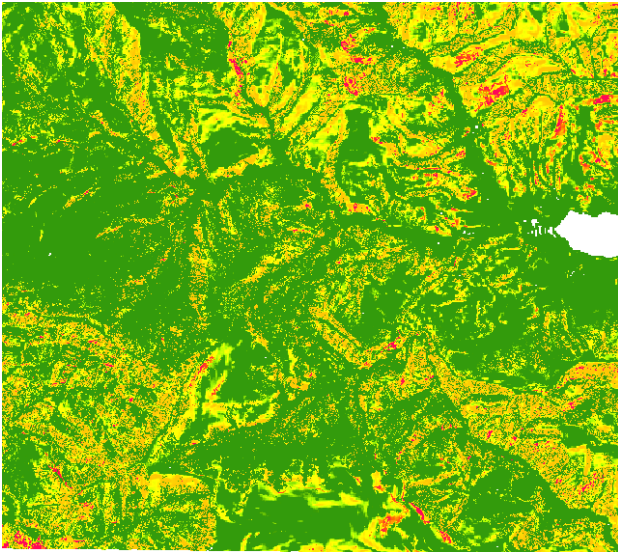


Figure 6: Result of landslide susceptibility based on maximum root cohesion and saturated conditions.

Comparing figures 3 and 6 indicates a good correspondence between those areas showing multiple slope failures and landslide susceptibility as mapped by the factor of safety computed from the infinite slope function. The error seems to be mainly in overestimating susceptibility in general, and some specific areas in particular. For example, the red spots in the bottom central part are not visible as landslide scars in the 2005 Quickbird image. The slopes there are rather steep however, ( $\sim 40^\circ$ ), and the land cover indicates grass/bare. Most slides occurred on the sites covered largely by grass, including mixtures of grass and shrubs, and grass and bare areas. Slope angle itself is also important, but there are areas in the study site with steep slopes ( $> 40^\circ$ ) that have not experienced sliding and are mapped as safe (green colour). Therefore, while slope is an important parameter, the slope alone cannot explain susceptibility.

A full sensitivity analysis has not been completed, but preliminary results suggest that the next most important factor to slope is cohesion. Changing the angle of internal friction yields a very similar result. For example, if  $\phi$  is given the lowest value for oaks and highest values for grass, the resulting map displays the same pattern. On the other hand, if low cohesion values are assigned to the oak trees and high values to the grassy areas, the pattern is reversed. Stable areas appear as susceptible to sliding, while failed areas appear as safe. Similarly, using the minimum values for root cohesion also increases the likelihood of mass wasting in apparently stable regions.

#### 4. CONCLUSIONS

While the results to date indicate the potential of this approach the accurate quantification of specific geotechnical parameters has proven quite challenging. While it appears that some areas are correctly quantified and identified with respect to susceptibility, there are other areas that should be safer than they appear. In the past the use of geotechnical methods for landslide susceptibility mapping has been limited due to the aforementioned lack of availability of geotechnical parameters. These limitations, given newly available coverages and

capabilities, seem to be less of an impediment. Moreover, this research suggests that satellite images can be successfully used to derive reasonable values for critical parameters in a geotechnical stability model, thereby increasing the utility of the geotechnical approach in landslide susceptibility mapping.

#### ACKNOWLEDGEMENTS

The authors want to thank San Francisco State University, the Geomorphic Computing Laboratory at the University of Iowa and the Iowa Hydraulics Institute, IIHR Hydroscience and Engineering at the University of Iowa for financial support.

#### REFERENCES

- American Society of Civil Engineers, 1994. Bearing capacity of soils. Technical Engineering and design guides as adapted from the US Army Corps of Engineers, No. 7, New York, ASCE Press.
- Ayalew, L., Yamagishi, H., 2005. The application of GIS-based logistic regression for landslide susceptibility mapping in the Kakuda-Yahiko Mountains, Central Japan. *Geomorphology*, 65 (1-2), pp. 15-31.
- Baeza, C., Corominas, J., 2001. Assessment of landslide susceptibility by means of multivariate statistical techniques. *Earth Surface Processes and Landforms*, 26(12), pp. 1251-1263.
- Blesius, L., Weirich, F., 2006. Estimation of geotechnical slope stability parameters for landslide susceptibility mapping using satellite imagery. In: *Abstracts of the Association of American Geographers 102th Annual Meeting*, Chicago, IL.
- Borga, M., Dalla Fontana, G., Da Ros, D., Marchi, L., 1998. Shallow landslide hazard assessment using a physically based model and digital elevation data. *Environmental Geology*, 35(2-3), pp. 81-88.
- Chung, C.-J.F., Fabbri, A.G., 1999. Probabilistic prediction models for landslide hazard mapping. *Photogrammetric Engineering & Remote Sensing*, 65(12), pp. 1389-1399.
- Das, B.M., 1997. *Advanced soil mechanics*. 2nd ed. Taylor & Francis, Washington DC.
- Das, B.M., 1998. *Principles of geotechnical engineering*. 4th ed. PWS Publishing Company, Boston.
- Guzzetti, F., Cardinali, M., Reichenbach, P., Carrara, A., 2000. Comparing landslide maps: a case study in the Upper Tiber River Basin, Central Italy. *Environmental Management*, 25(3), pp. 247-263.
- Hanes, T.L., 1988. California Chaparral. In: Barbour, M.G., Major, J., (Eds.): *Terrestrial vegetation of California*. California Native Plant Society Special Publication Nr. 9, Sacramento, pp. 886-892.
- Hellmers, H., Horton, J.S., Juhren, G., O'Keefe, J., 1955. Root systems of some chaparral plants in southern California. *Geology*, 36(4), pp. 667-678.

- Hengchaovanich, D. Nilaweera, N.S., 1996. An assessment of strength properties of Vetiver Grass roots in relation to slope stabilization. In: Proc. 1st International Conference on Vetiver. Chiang Rai, Thailand, pp. 153-158.
- Holland, V.L., 2005. Coastal Oak Woodland. <http://dfg.ca.gov/biogeodata/cwhr/pdfs/cow.pdf> (accessed 6 Apr. 2009).
- Kurupparachchi, T., Wyrwoll, K.-H., 1992. The role of vegetation clearing in the mass failure of hillslopes: Moresby Range, Western Australia. *Catena*, 19(2), No. pp. 193-208.
- Mooney, H.A., 1988. Southern Coastal Scrub. In: Barbour, M.G. & J. Major (eds.): *Terrestrial vegetation of California*. California Native Plant Society Special Publication Nr. 9, Sacramento, pp. 471-489.
- NRCS, Natural Resource Conservation Survey, 2009. Web Soil Survey. <http://websoilsurvey.nrcs.usda.gov/app/HomePage.htm> (accessed 6 Apr. 2009).
- Pavlik, J., Muick, P., Johnson, S., Popper, M., 1991. *Oaks of California*. Cachuma Press, Los Olivos
- Preston, N.J., Crozier, M.J., 1999. Resistance to shallow landslide failure through root-derived cohesion in East Coast Hill Country soils, North Island, New Zealand. *Earth Surface Processes and Landforms*, 24(8), pp. 665-675.
- Rice, R.M., Corbett, E.S., Bailey, R.G., 1969. Soil slips related to vegetation, topography, and soils in Southern California. *Water Resources Research*, 5(3), pp. 647-659.
- Saboya, F., Da Gloria Alves, M., Pinto, W.D., 2005. Assessment of failure susceptibility of soil slopes using fuzzy logic. *Engineering Geology*, 86(4), pp. 211-224.
- Sarkar, S., Kanungo, D.P., 2004. An integrated approach for landslide susceptibility mapping using remote sensing and GIS. *Photogrammetric Engineering & Remote Sensing*, 70(5), pp. 617-625.
- Schlesinger, W.H., Gill, D.S. 1980. Biomass, production, and changes in the availability of light, water, and nutrients during the development of pure stands of the chaparral shrub, *Ceanothus Megacarpus*, after fire. *Ecology*, 61(4), pp. 781-789.
- Sidle, R.C., 1992. A theoretical model of the effects of timber harvesting on slope stability. *Water Resources Research*, 28(7), pp. 1897-1910.
- State of California DOT (1990): Trenching and shoring manual. <http://www.dot.ca.gov/hq/esc/construction/manuals/OSCCompleteManuals/TrenchingandShoringManualRev12.pdf> (accessed 14 April 2009).
- Terlien, M.T.J., 1998. The determination of statistical and deterministic hydrological landslide-triggering thresholds. *Environmental Geology*, 35(2-3), pp. 124-130.
- Terzaghi, K., R.B. Peck, Mesri, G., 1996. *Soil mechanics in engineering practice*. 3rd ed. John Wiley & Sons, New York.
- Van Westen, C.J., Terlien, M.T.J., 1996. An approach towards deterministic landslide hazard analysis in GIS. A case study from Manizales (Colombia). *Earth Surface Processes and Landforms*, 21(9), pp. 853-868.
- Wu, T.H., 1995. Slope stabilization. In: Morgan, R.P.C. and R.J. Rickson (eds.): *Slope stabilization and erosion control: A Bioengineering approach*. E&FN Spon/Chapman and Hall, London
- Wu, W., Sidle, R.C., 1995. A distributed slope stability model for steep forested basins. *Water Resources Research*, 31(8), pp. 2097-2110.
- Yu, Q., Gong, P., Clinton, N., Kelly, M., Schirokauer, D., 2006. Object-based detailed vegetation classification with airborne high spatial resolution remote sensing imagery. *Photogrammetric Engineering & Remote Sensing*, 72(7), pp. 799-811.